Academic Journal of Science and Technology
ISSN: 2771-3032 | Vol. 13, No. 3, 2024

Experimental Study of a Schiff Base as Corrosion Inhibitor for Mild Steel in 1M HCl

Jing Zhou[1], Yue Li[1,*], Yutong Wei[1], Chaozheng Long[1], Bin Yi[1], Xiaoli Sun[1], Boyan Ren[1], Keqian Deng[1], Fangde Fan[1]

[1] Dazhou Market Supervision and Administration Bureau, Dazhou 635000, China

[*] Corresponding authors: 1498418249@qq.com (Yue Li)

Abstract: In this paper, salicylaldehyde ethylenediamine Schiff base (SESB) was prepared by reaction of salicylaldehyde and ethylenediamine at 60℃ for 4 h. The structure of SESB was characterized by hydrogen magnetic resonance spectroscopy. The corrosion inhibition effect of SESB on mild steel in 1mol L^{-1}HCl was studied by weight loss method and electrochemical method. The results showed that the corrosion inhibition effect of SESB on mild steel at 1mol L^{-1} HCl was negatively correlated with the test temperature at 25℃ to 45℃, and positively correlated with the concentration of SESB at 0mmol L^{-1} to 5mmol L^{-1}. The results showed that the maximum corrosion inhibition efficiency of SESB at 25℃, 30℃, 35℃, 40℃ and 45℃ were 70.73%, 58.42%, 54.68%, 37.73% and 25.12%, respectively. The results of electrochemical impedance test and electrochemical polarization test show that SESB can not only inhibit the anode metal dissolution of mild steel in 1mol L^{-1} HCl, but also inhibit the cathode hydrogen precipitation, which is a mixed corrosion inhibitor.

Keywords: Salicylaldehyde ethylenediamine, double Schiff base, corrosion inhibitor, mild steel.

1. Introduction

Metal or metal-based alloys are one of the most widely used materials, especially carbon steel, due to its good ductility and plasticity, can better solve the material continuity problem caused by special structural requirements [1-4]. These are widely used in oil well acidification in the process of oil and gas exploitation, pickling in the cleaning process of chemical equipment and ships [5,6]. However, carbon steel has a higher degree of freedom, which increases the possibility of corrosion by the environment. Especially in the acidification of oil and gas Wells and pickling of chemical equipment, the metal corrosion is more serious. The occurrence of corrosion behavior will reduce the service performance and shorten the service life of metal equipment [7], and even cause environmental pollution, fire, explosion and other catastrophic accidents, bringing huge economic losses. According to statistics, the direct economic loss caused by metal corrosion accounts for 3 % of GDP of various countries every year [8,9]. Therefore, it is urgent and necessary to study efficient, convenient, low cost and environmental protection corrosion inhibition means of carbon steel, especially for the pickling process of carbon steel equipment and pipelines.

Organic corrosion inhibitors mainly include organic amines, imidazoline, quaternary ammonium salts, natural plant extracts and so on. Unfortunately, the structure of efficient organic corrosion inhibitors mainly contains P, S and other elements, and lacks environmental friendliness. At the same time, there are shortcomings in the long-term performance of plant natural product extracts, solvent consumption during extraction and the determination of main components. [10-13]

The aim of this work is to synthesize an environmental protection, high efficiency and low-cost corrosion inhibitor for mild steel. Most of the organic corrosion inhibitors contain S, N, O, P and other atoms in structure. The main mechanism is to form coordination bonds between the lone pair electrons carried by these atoms when forming compounds and the empty orbital of the metal, thus forming an anti-corrosion film covered by the corrosion inhibitor on the surface of the metal. Salicylaldehyde ethylenediamine Schiff base (SESB) contains two N atoms in composition, and its presence ensures that SESB and iron atoms can form chelates containing two coordination bonds, enhancing the stability of the complex. The O atom, which is structurally far from the N atom, also has lone pairs of electrons and can form coordination bonds with the metal, which further enhances the adsorption capacity of the complex. SESB avoids the presence of harmful elements such as P and S in its structure and reduces the pollution to the environment during use.

2. Materials and Methods

2.1. Materials

All chemicals and solvents are derived from Shanghai Titan's AR grade products without further purification. The composition of mild steel sample used in this study is: C, 0.21%; Si, 0.45%; Mn, 0.19%; P and S, < 0.01%; the rest are Fe elements. The mild steel plate was divided into 2.5cm × 0.5cm × 5.0cm samples for weight loss measurement.

2.2. Synthesis of SESB

3.89ml of salicylaldehyde was diluted with 15ml of anhydrous ethanol in 250ml three-neck flask, and then 1.24ml of ethylenediamine was slowly added to the salicylaldehyde dilution solution through a constant pressure funnel, and the reaction was maintained at 60℃ for 4 hours (Fig 1). After the reaction, the mass of SESB was 4.3484 g and the yield was about 87%. The structure of the final product was identified by ^{1}H-NMR spectroscopy, as shown in Fig 2.

^{1}H NMR (600 MHz, DMSO-d_6 ppm): ^{1}H NMR (600 MHz, DMSO-d_6) δ 13.39 (s, 2H), 8.59 (s, 2H), 7.42 (dd, J = 7.6, 1.7 Hz, 2H), 7.32 (ddd, J = 8.7, 7.3, 1.7 Hz, 2H), 6.95 – 6.81 (m，4H), 3.92 (s, 4H). [14-16]

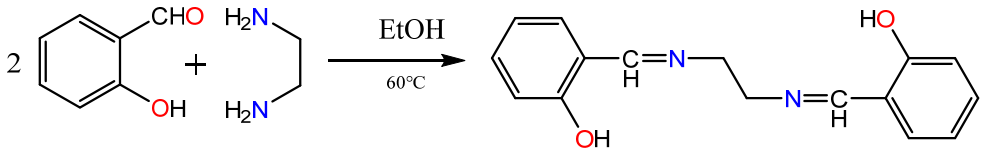

Figure 1. Scheme of reaction

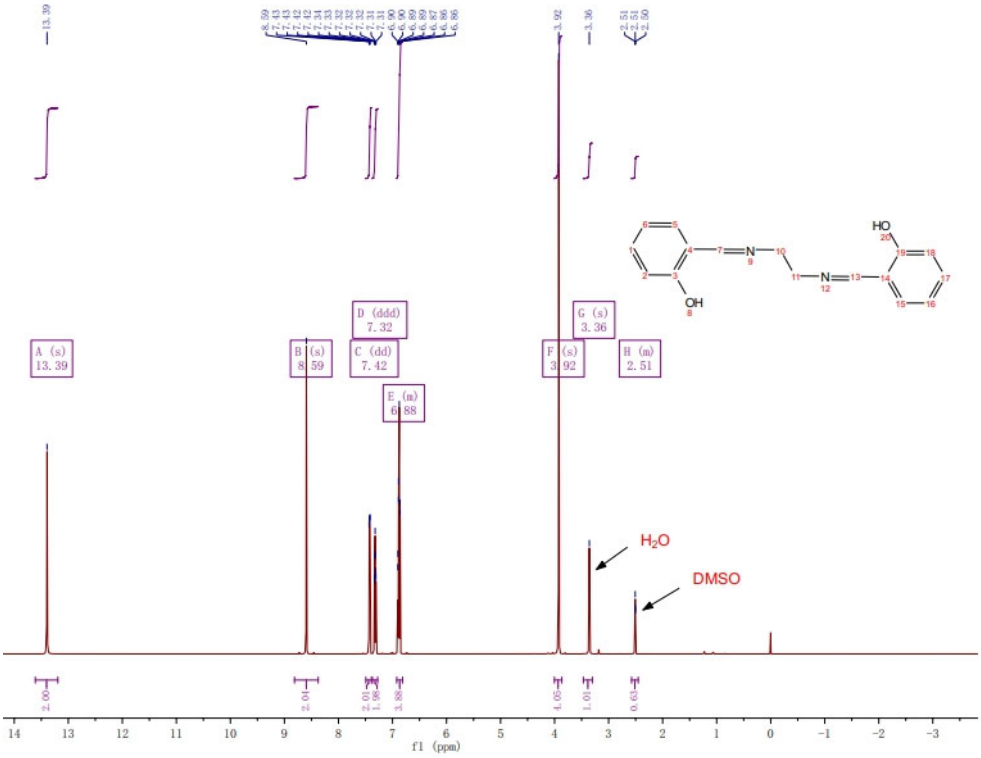

Figure 2. The 1H-NMR spectroscopy of SESB.

2.3. Inhibitor performance test

2.3.1. Electrochemical test

The corrosion inhibition performance of SESB on mild steel was evaluated by electrochemical (three-electrode system, CHI660E) tests. All electrochemical measurements were carried out with standard three electrodes, in which Pt electrode was used as the auxiliary electrode, saturated calomel electrode as the reference electrode, and carbon steel electrode as the working electrode. All potentials were referencing saturated calomel electrode, and the effective exposure area of the working electrode was 0.196 cm^2. Before measurement, the prepared working electrode parameters were set to 1200s, the impedance frequency was set to 10^{-2} to 10^5Hz, the amplitude was set to 5mV, the polarization curves were obtained at a scan rate of 0.5mV/s in the range of (-0.25 V) - (+0.25 V) of the open termination potential. After the sample is immersed in the solution and the circuit is stabilized, the corrosion potential is measured (open circuit OCPT is selected). After the open-circuit potential measurement, the Tafel curve test was carried out to obtain the electrochemical impedance spectrum and its data, and the potentiodynamic polarization curve and its data.

2.3.2. Gravimetric analysis

The corrosion inhibition efficiency of SESB at different concentrations at 25℃, 30℃, 35℃, 40℃ and 45℃ was studied by static weight loss method. First of all, before the start of the experiment, the steel sheet was polished to 1200#, polished until the surface of the steel sheet was smooth without obvious scratches such as mirror smooth, and its length, width and height were measured and recorded after washing, drying and cooling by distilled water and acetone in turn, and the electronic balance was used to weigh and record its quality. SESB was added to 1mol L^{-1} HCl according to the concentration gradient, sealed and placed in a constant temperature water bath for 30 minutes, and then the measured steel sheet was soaked at the set temperature for 4 hours. In order to eliminate accidental errors caused by the experiment, three sets of parallel experiments were set to ensure the accuracy of the experiment. After the reaction, the steel sheet was cleaned, dried, cooled, weighed and recorded with distilled water and acetone in turn. The corrosion rate was calculated by equation 1 based on the mass difference Δm, surface area s and reaction time t before and after drawing out the steel block, and then the corrosion inhibition efficiency of SESB with different concentrations was calculated from Equations (1) and (2) [17]:

$$v = \frac{m_0 - m}{st} = \frac{\Delta m}{st} \quad (1)$$

$$\eta_W\ (\%) = \frac{v - v_0}{v} \quad (2)$$

Where m represents the mass of the steel block after the test, and the unit is g; m_0 represents the mass of the steel block before the experiment, and the unit is g; v represents the corrosion rate of the experimental group, the unit is g h^{-1} cm^{-2}; v_0 represents the corrosion rate of the steel block in the control group, and the unit is g h^{-1} cm^{-2}. η_W indicates the corrosion inhibition efficiency.

3. Results and Discussion

3.1. Electrochemical impedance analysis

Figs 3-7 show the Nyquist and bode graphs obtained by SESB at different temperatures. From the shape change of Nyquist plot, it can be seen that the radius of Nyquist curve gradually increases with the addition of SESB. This is mainly because the corrosion inhibitor SESB is adsorbed on the surface of mild steel through adsorption, forming a protective film, increasing the electrical conductivity of the surface of mild steel, making its impedance increase. It can be obviously found from the figure that the shape of the curve does not change significantly with the addition of SESB, indicating that the addition of corrosion inhibitor does not change the corrosion mechanism of mild steel in 1mol L^{-1} HCl. On the other hand, by comparing the bode diagram, it can be observed that the bode curve has only one peak, indicating that the reaction has only one time constant. In summary, the corrosion inhibition mechanism of SESB is simply adsorbed on the surface of mild steel and plays a role in corrosion inhibition through charge transfer control. Compared with Nyquist plots at different temperatures, it can be found that the radius of Nyquist curve increases gradually with the increase of temperature, indicating that the ability of SESB to inhibit the corrosion of mild steel in 1mmol L^{-1} HCl decreases with the increase of temperature. At the same time, it is found that the circle presented by Nyquist curve is not a perfect semi-circle, which may be caused by the electrode is not polished smoothly.

In addition, R(QR) equivalent circuit diagram was used in this experiment to analyze the electrochemical impedance data, and the fitting parameters in the following table were obtained, as shown in Table 1. In the table, T represents temperature, and the unit is °C; C_{inh} represents the concentration of corrosion inhibitor, the unit is mmol L^{-1}; R_s indicates the resistance of the solution, expressed in Ω cm^2. R_{ct} indicates the mass transfer resistance, and the unit is Ω cm^2. n is the dispersion constant; Y_0 is the proportional constant, the unit is $\mu\Omega^{-1}S^n.\ m^{-2}$; χ^2 indicates goodness of fit; η_E indicates the corrosion inhibition efficiency.

The corrosion inhibition efficiency (η_E) and the double-layer capacitance are calculated by equations (3).

$$\eta_E = \left(1 - \frac{R_{ct}^0}{R_{ct}}\right) \times 100\% \quad (3)$$

η_E represents the corrosion inhibition efficiency; R_{ct} indicates that the charge transfer resistance after the addition of corrosion inhibitor is the mass transfer resistance, and the unit is Ω cm^2. R_{ct}^0 represents the charge transfer resistance when no corrosion inhibitor is added, and the unit is Ω cm^2. Through this formula, we can estimate the corrosion inhibition efficiency of the inhibitor[18, 19].

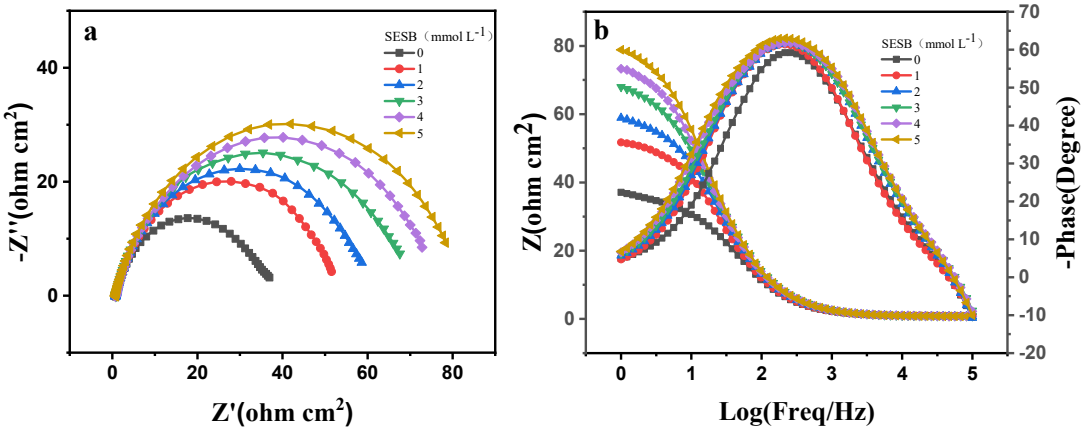

Figure 3. Nyquist diagram (a) and bode diagram (b) of SESB impedance at 45°C

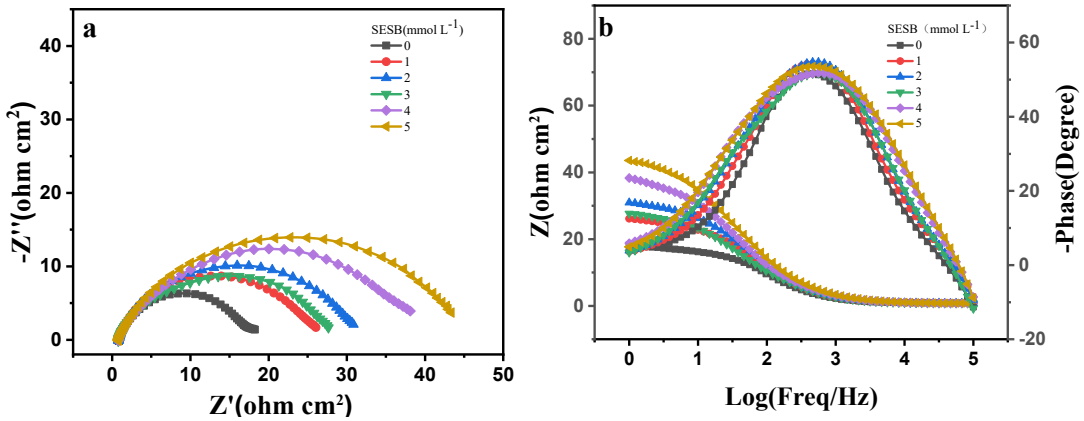

Figure 4. Nyquist diagram (a) and bode diagram (b) of SESB impedance at 45°C

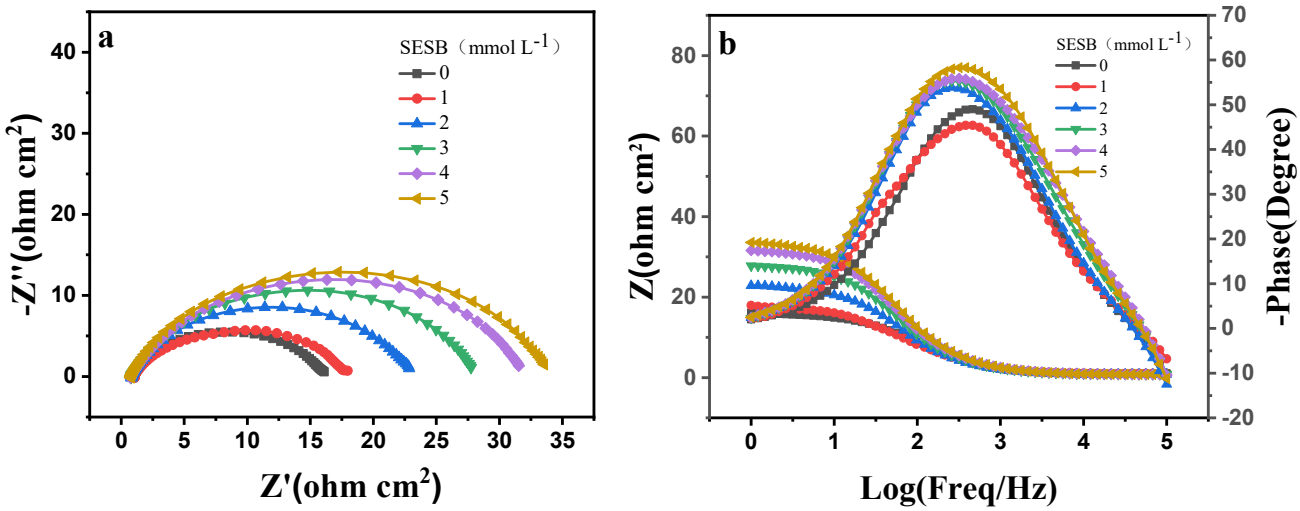

Figure 5. Nyquist diagram (a) and bode diagram (b) of SESB impedance at 45℃

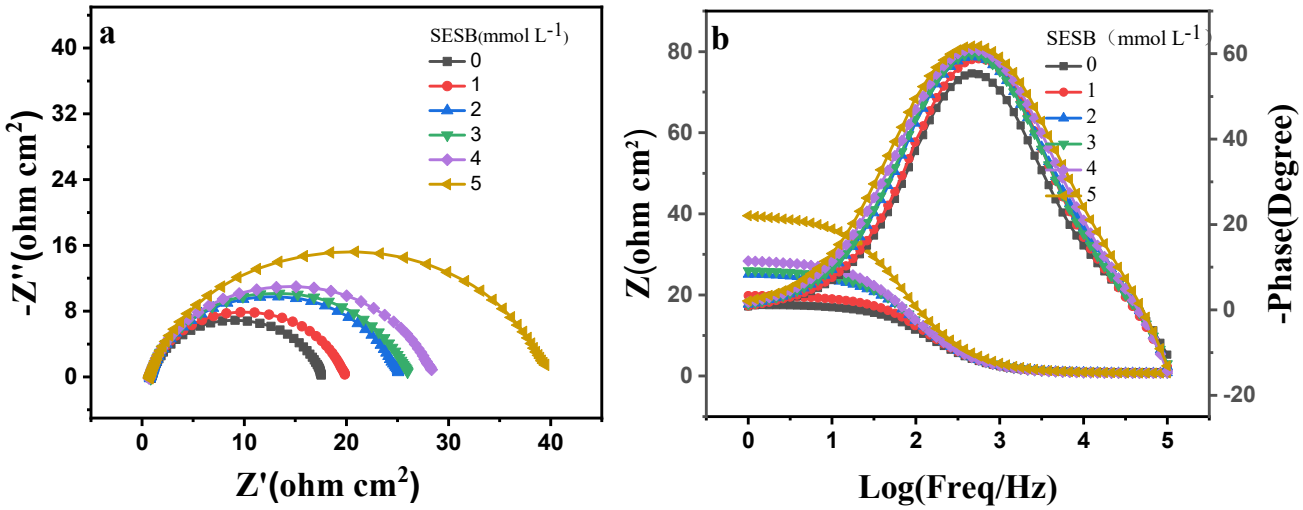

Figure 6. Nyquist diagram (a) and bode diagram (b) of SESB impedance at 45℃

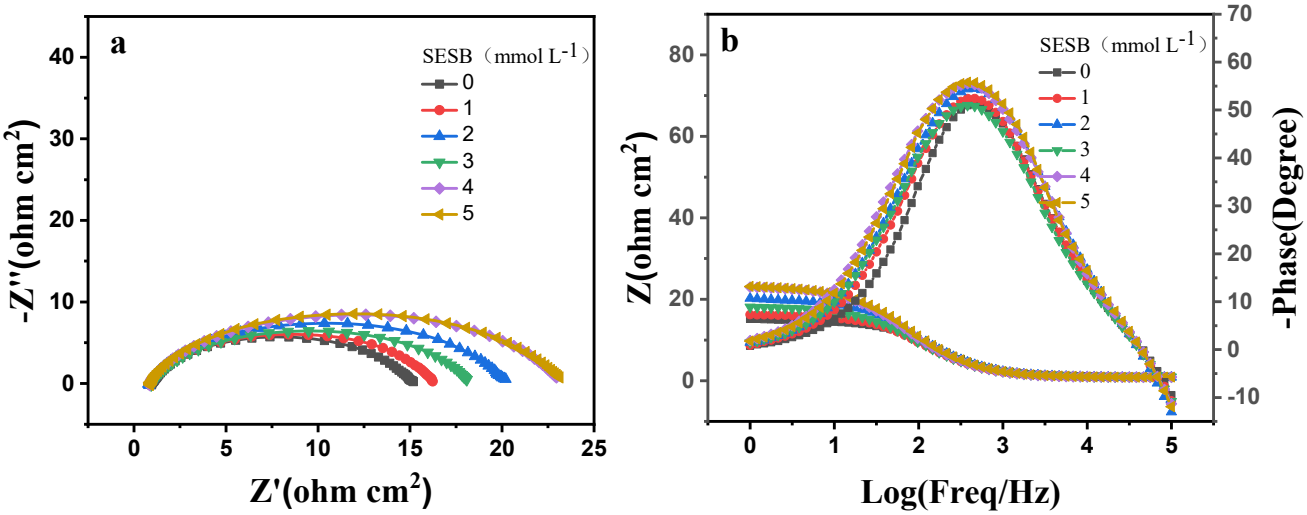

Figure 7. Nyquist diagram (a) and bode diagram (b) of SESB impedance at 45℃

Table 1. Fitting data of R(QR) equivalent circuit at 25℃, 30℃, 35℃, 40℃ and 45℃

T (℃)	C_{inh} (mmol L^{-1})	R_s(Ω cm^2)	R_{ct}(Ω cm^2)	n	Y_0(μΩ^{-1}S^n.cm^{-2})	χ^2	η_E(%)
25	0	0.8622	35.63	0.8365	368	0.002812	
	1	0.9283	51.62	0.8434	344	0.002164	30.98
	2	0.7763	59.04	0.8262	350	0.002881	39.65
	3	0.8096	68.33	0.8164	355	0.002224	47.86
	4	0.7748	75.29	0.8114	370	0.002293	52.68
	5	0.7652	80.92	0.8202	346	0.002640	55.97
30	0	0.8634	16.68	0.8378	363	0.003544	
	1	0.8626	24.49	0.8159	363	0.002523	31.89
	2	0.7994	29.35	0.7994	392	0.003836	43.17
	3	0.7597	26.37	0.7678	545	0.006186	36.75
	4	0.7477	37.67	0.7431	559	0.004396	55.72
	5	0.7525	43.10	0.7516	447	0.004004	61.30
35	0	0.9264	14.94	0.8286	412	0.002704	
	1	1.0270	16.70	0.7761	654	0.002002	10.54
	2	0.8235	22.21	0.8269	448	0.003710	32.73
	3	0.7817	27.79	0.8125	422	0.003160	46.24
	4	0.7591	31.81	0.8031	402	0.003514	53.03
	5	0.7603	33.29	0.8313	322	0.003255	55.12
40	0	0.9384	16.55	0.8912	200	0.002340	
	1	0.8262	18.74	0.9045	169	0.003789	11.69
	2	0.8049	24.06	0.8790	198	0.003886	31.21
	3	0.8537	24.80	0.8890	185	0.003463	33.27
	4	0.7150	27.36	0.8753	207	0.004577	39.51
	5	0.7702	38.52	0.8604	188	0.004232	57.04
45	0	0.9779	14.08	0.8672	254	0.002229	
	1	0.8726	15.35	0.8548	323	0.002945	8.27
	2	0.2210	19.19	0.8473	312	0.004096	26.63
	3	0.9556	17.14	0.8339	382	0.002745	17.85
	4	0.8551	22.05	0.8446	343	0.002879	36.15
	5	0.8650	22.16	0.8487	143	0.003159	36.46

As can be seen from the data in Table 1, the R_{ct} value of mass transfer resistance on the surface of mild steel gradually increases with the increase of the concentration of corrosion inhibition SESB, and the corrosion inhibition efficiency *(η_E)* of SESB generally increases. This is mainly because SESB uses heteroatom lone pair electrons and unsaturated π electrons in the structure to bind to the empty orbitals of Fe atoms on the surface of mild steel, which prevents the surface of mild steel from contacting with acidic media through adsorption film formation, and plays a role in corrosion inhibition. Therefore, as the concentration of the inhibitor increases, the protective layer formed by SESB on the surface of the mild steel becomes more complete and denser, thus improving its corrosion inhibition performance. At different temperatures, the corrosion inhibition efficiency of SESB decreased with the increase of temperature. This may be because with the increase of temperature, the H^+ activity of acid medium system is enhanced, the cathodic corrosion of mild steel is accelerated, and the generation of hydrogen bubbles is increased, resulting in the desorption of corrosion inhibitors. It can be seen from η_E(%) that the corrosion inhibition effect basically reaches the maximum value when the corrosion inhibitor concentration reaches 5 mmol L^{-1}. Below 40℃, the corrosion inhibition effect of the corrosion inhibitor is more stable, and the highest corrosion inhibition efficiency of the corrosion inhibitor is 61.30%. It shows that the corrosion inhibitor can obviously inhibit the corrosion of mild steel in 1mmol L^{-1} HCl, and has high application value and academic value.

3.2. Tafel test

Electrochemical potentiodynamic polarization spectrum is an important part of electrochemical testing and a powerful supplement to electrochemical impedance spectrum. The data obtained from the analysis of the spectra of electrochemical dynamic polarization curves is an important reference for judging whether the electrochemical impedance test results are correct [15]. Fig 8 shows the potentiodynamic polarization curves at different temperatures. By observing Fig 8, it can be found that with the addition of corrosion inhibitor SESB, both cathode and anode of the potentiodynamic polarization curve have significant negative shifts, indicating that SESB belongs to a mixed type of corrosion inhibitor of cathode and anode. In addition, we can

also find from the figure that the overall negative shift of the polarization curve gradually decreases with the increase of temperature, indicating that the average corrosion inhibition efficiency of different concentrations of SESB gradually decreases with the increase of temperature. At the same time, it can be clearly found from Fig 8 that the addition of corrosion inhibitor SESB does not cause significant shift in polarization potential, which further proves that the inhibitor is a mixed corrosion inhibitor. The specific parameters of the polarization curve are listed in Table 2, where T represents temperature; C_{inh} stands for corrosion inhibitor concentration; I_{corr} stands for corrosion current; β_a and $-\beta_c$ represent the absolute values of the anode slope and the cathode slope of the Tafel curve respectively. E_{corr} represents corrosion potential; η_P indicates the corrosion inhibition efficiency. The corrosion inhibition efficiency (η_p) and the double-layer capacitance are calculated by equations (4).

$$\eta_p = \left(1 - \frac{I_{corr}}{I_{corr}^0}\right) \times 100\% \quad (4)$$

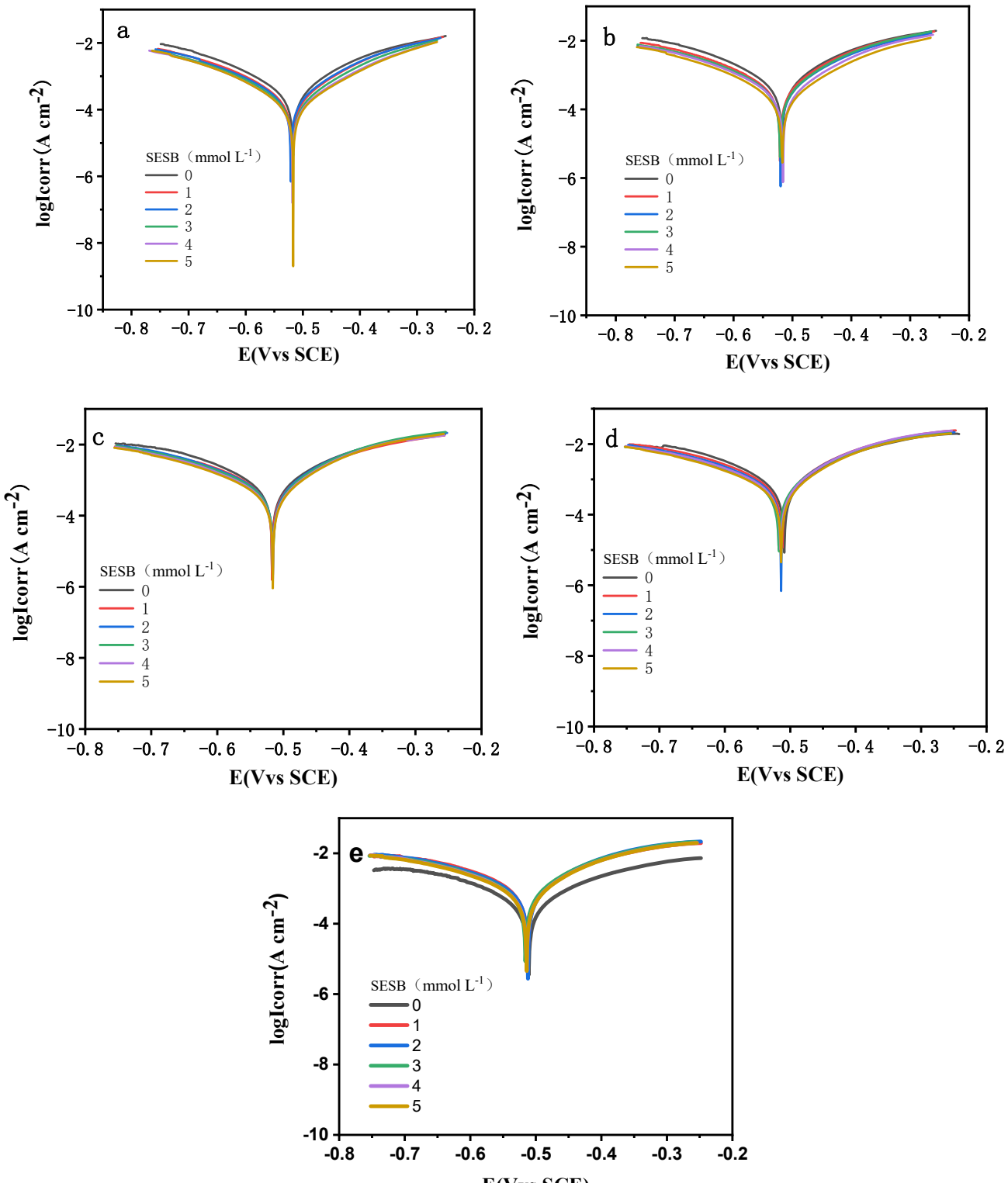

Figure 8. The Tafel polarization plots of mild steel at 25°C, 30°C, 35°C, 40°C and 45°C at 1.0 M HCl with different SESB concentrations.

Table 2. The date of Tafel polarization plots of mild steel at 25℃, 30℃, 35℃, 40℃ and 45℃ at 1.0 M HCl with different SESB concentrations.

T（℃）	C_{inh} (mmol L^{-1})	I_{corr} (μA cm^{-2})	β_a (mv dec^{-1})	$-\beta_c$ (mv dec^{-1})	E_{corr}(V)	η_p(%)
25	0	328.0	8.634	8.063	-0.517	0
	1	213.7	9.480	7.927	-0.518	34.85
	2	222.8	9.351	7.502	-0.521	32.07
	3	164.9	9.622	8.006	-0.518	49.73
	4	139.0	9.446	8.308	-0.518	57.62
	5	132.3	9.430	8.414	-0.517	59.66
30	0	575.0	8.101	7.527	-0.518	0
	1	448.7	8.696	7.141	-0.521	21.97
	2	387.7	8.771	6.963	-0.520	32.57
	3	372.7	9.117	7.162	-0.521	35.18
	4	296.5	9.242	7.308	-0.516	48.43
	5	227.7	9.204	7.438	-0.517	60.40
35	0	731.8	7.877	7.213	-0.517	0
	1	660.5	8.005	6.485	-0.517	9.74
	2	539.3	8.415	8.836	-0.516	26.31
	3	450.0	8.881	8.694	-0.516	38.51
	4	431.4	10.729	7.019	-0.516	41.05
	5	372.2	12.018	6.864	-0.516	49.14
40	0	837.1	7.550	7.056	-0.509	0
	1	820.8	8.041	6.600	-0.512	1.95
	2	657.6	10.109	6.577	-0.514	21.44
	3	624.1	9.071	6.746	-0.517	25.44
	4	596.0	10.599	6.418	-0.515	28.80
	5	461.1	11.821	6.542	-0.514	44.92
45	0	1133.0	2.216	2.864	-0.511	0
	1	1072.0	7.317	5.970	-0.512	5.38
	2	823.2	10.876	5.803	-0.512	27.34
	3	975.7	7.705	5.900	-0.516	13.88
	4	867.4	7.788	5.981	-0.514	23.44
	5	822.9	7.999	6.112	-0.514	27.37

The corrosion inhibition performance of SESB in 1mol L^{-1} HCl was determined by analyzing the corrosion current I_{corr} of the dynamic polarization curve, the Tafel slope $_{\beta c}$ of cathode and anode, and the corrosion potential E_{corr} of β_a. Table 2 shows the effects of SESB concentrations at different temperatures (25℃, 30℃, 35℃, 40℃, 45℃) on the potentiodynamic polarization parameters of mild steel in 1mol L^{-1} HCl. It is evident from the data in Table 2 that with the increase of the concentration of corrosion inhibitor SESB, the I_{corr} value of the surface corrosion current of mild steel gradually decreases, indicating that the addition of corrosion inhibitor SESB can significantly inhibit the corrosion behavior of the surface of mild steel in 1mol L^{-1} HCl. On the other hand, with the increase of temperature, the corrosion current on the surface of mild steel showed an overall upward trend, and the reduction degree of corrosion current gradually decreased with the increase of corrosion inhibitor concentration, which was consistent with the change trend of electrochemical impedance. This is mainly because with the increase of temperature, the activity of the acidic medium system is enhanced, and the conductivity of the acidic system is enhanced, which promotes the corrosion process of mild steel in 1mol L^{-1} HCl. It can be seen from Table 2 η_p(%) data that the maximum corrosion inhibition efficiency of SESB is 60.40%, which is very close to the electrochemical impedance data, indicating that the data is highly reliable.

3.3. Gravimetric analysis

Static weight loss method is a more realistic experimental method than electrochemical method, and the corrosion inhibition efficiency of SESB in 1mol L^{-1} HCl can be better measured by comparing corrosion rates at different temperatures and concentrations [18]. Fig. 9 shows the effect of SESB concentration on corrosion behavior of mild steel in 1mol L^{-1} HCl at different temperatures. Specific parameters are listed in Table 3, where V represents corrosion rate in g h^{-1} cm^{-2}, η_W represents corrosion inhibition efficiency, and θ represents corrosion inhibitor coverage. It can be seen from Fig. 8 that with the increase of corrosion inhibition concentration, the corrosion rate of mild steel in 1mol L^{-1} HCl gradually decreases, and the corrosion inhibition efficiency of SESB gradually increases. It can be obviously found from the figure that when the concentration of corrosion inhibitor is 1mmol L^{-1}, the influence on the corrosion behavior of mild steel is most obvious. When the concentration of corrosion inhibitor is 2mmol L^{-1}, the curve tends to be horizontal, indicating that the concentration of corrosion inhibitor has little influence on the corrosion behavior of mild steel. This is mainly because the surface area of the test mild steel sample is limited, and the corrosion inhibitor is saturated on its surface, so that the correlation between the corrosion inhibition effect and the corrosion inhibitor concentration is reduced. It can be seen from the data in Table 3 that the frontal coverage of corrosion inhibitor on the surface of mild steel is

positively correlated with the concentration of corrosion inhibitor. This is also one of the main reasons why the corrosion inhibition effect of corrosion inhibitor is positively correlated with its concentration. On the other hand, the high consistency between the weight loss inhibition efficiency and the electrochemical data proves the experimental feasibility and data reliability of this experiment.

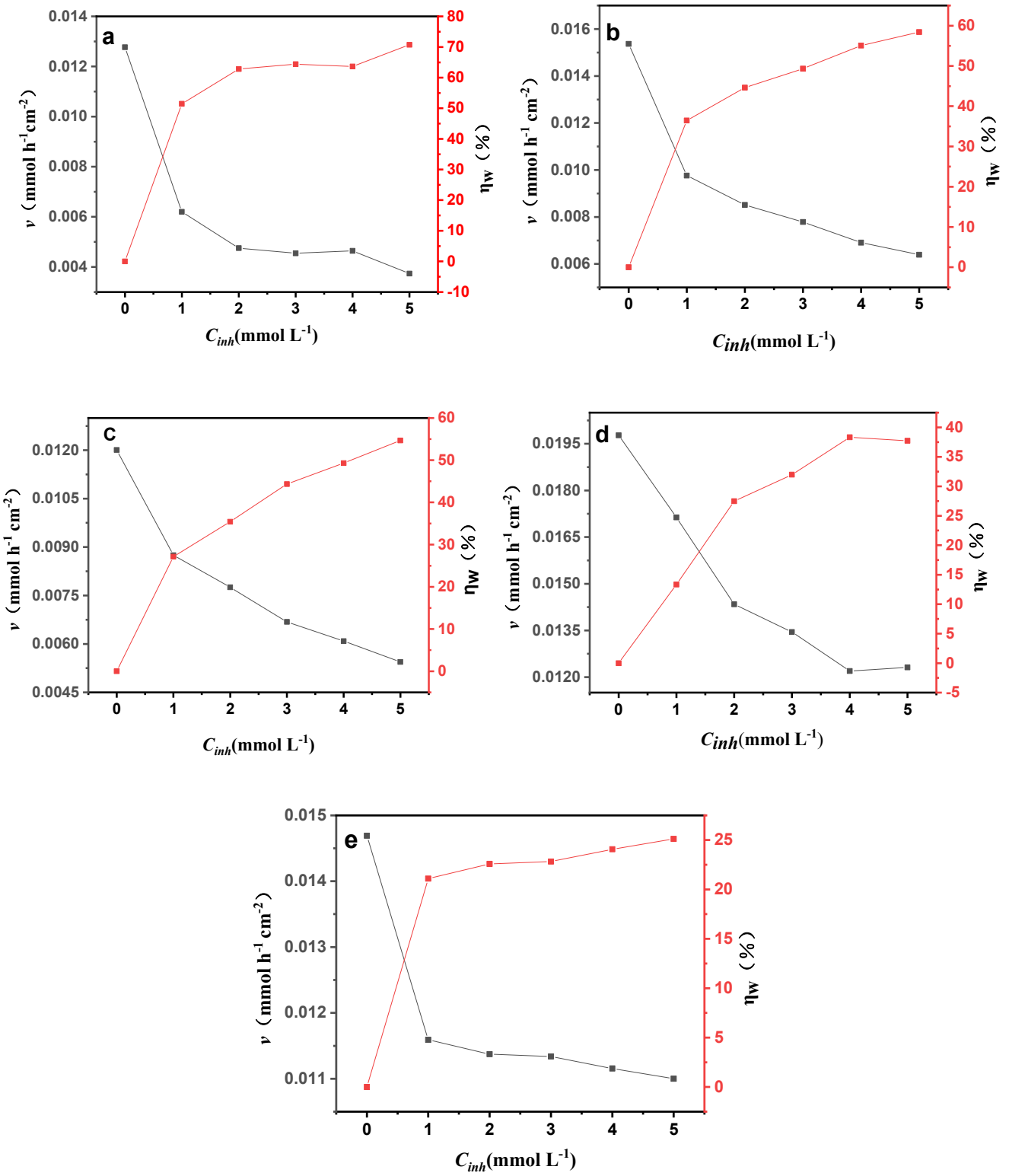

Figure 8. The relationship between SESB corrosion inhibition efficiency and concentration and test temperature

Table 3. Weight loss test results

T(℃)	c_{inh} (mmol L^{-1})	v (g h^{-1} cm^{-2})	η_W (%)	θ
25	0	0.01277	0.00	0.00
	1	0.00620	51.44	0.51
	2	0.00475	62.79	0.63
	3	0.00455	64.40	0.64
	4	0.00464	63.63	0.64
	5	0.00374	70.73	0.71
30	0	0.01537	0.00	0.00
	1	0.00977	36.46	0.36
	2	0.00851	44.61	0.45
	3	0.00779	49.33	0.49
	4	0.00691	55.06	0.55
	5	0.00639	58.42	0.58
35	0	0.01201	0.00	0.00
	1	0.00832	27.14	0.27
	2	0.00808	35.43	0.35
	3	0.00618	44.35	0.44
	4	0.00480	49.30	0.49
	5	0.00478	54.68	0.55
40	0	0.01977	0.00	0.00
	1	0.01713	13.35	0.13
	2	0.01434	27.47	0.27
	3	0.01345	31.98	0.32
	4	0.01220	38.32	0.38
	5	0.01231	37.73	0.38
45	0	0.01469	0.00	0.00
	1	0.01159	21.10	0.21
	2	0.01400	22.58	0.23
	3	0.01189	22.82	0.23
	4	0.01173	24.06	0.24
	5	0.01063	25.12	0.25

3.4. Adsorption and thermodynamic parameter study

To better describe the interaction between SESB and mild steel at different temperatures and concentrations, and to explore the adsorption effect of SESB on mild steel, we chose Langmuir adsorption isotherm formula to fit and studied it by thermodynamic method. Langmuir isothermal formula is shown in equation (5), and the relationship between adsorption equilibrium constant K_{ads} and adsorption free energy ΔG_{ads} is shown in equation (6):

$$\frac{C}{\theta} = C + \frac{1}{K_{ads}} \tag{5}$$

$$K_{ads} = \frac{1}{55.5} exp\left(\frac{\Delta G_{ads}}{RT}\right) \tag{6}$$

Where C represents the concentration of corrosion inhibitor added; θ represents the coverage rate of the added corrosion inhibitor on the surface of mild steel; R is the gas constant; T is the absolute temperature; 55.5 is the concentration of water in the solution.

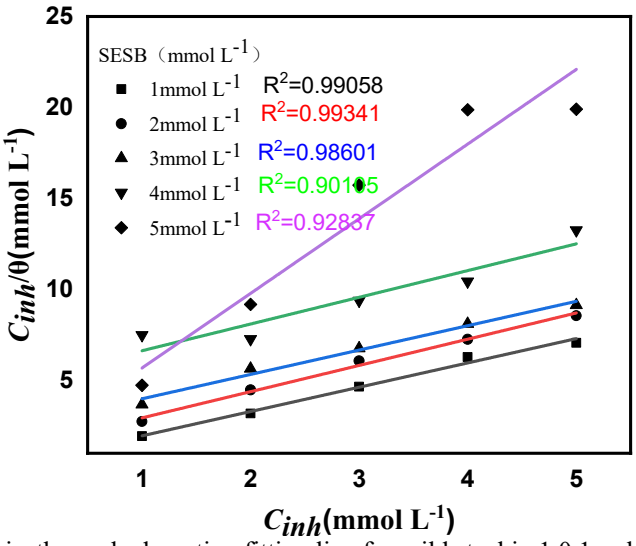

Figure 9. Langmuir isothermal adsorption fitting line for mild steel in 1.0 1mol L^{-1} HCl with SESB

The relationship between C and C/θ is shown in Fig. 9. Through fitting, we can see that the fitting linear correlation coefficients are all higher than 0.99 when the SESB concentration is 1 and 2mmol L^{-1}, and the fitting correlation coefficients are also higher than 0.90 when the SESB concentration is 3, 4 and 5mmol L^{-1}. Through the above data, we can find that C and C/θ have a good linear relationship in general.

4. Conclusion

In this paper, salicylaldehyde ethylenediamine Schiff base (SESB) was prepared by reaction of salicylaldehyde and ethylenediamine at 60℃ for 4 h. The structure of SESB was characterized by hydrogen magnetic resonance spectroscopy. The corrosion inhibition effect of SESB on mild steel in 1mol L^{-1} HCl was studied by weight loss method and electrochemical method. The results showed that the corrosion inhibition effect of SESB on mild steel at 1mL^{-1} HCl was negatively correlated with the test temperature at 25℃ to 45℃, and positively correlated with the concentration of SESB at 0mL-1 to 5mL^{-1}. The results showed that the maximum corrosion inhibition efficiency of SESB at 25℃, 30℃, 35℃, 40℃ and 45℃ were 70.73%, 58.42%, 54.68%, 37.73% and 25.12%, respectively. The results of electrochemical impedance test and electrochemical polarization test show that SESB can not only inhibit the anode metal dissolution of mild steel in 1mol L^{-1} HCl, but also inhibit the cathode hydrogen precipitation, which is a mixed corrosion inhibitor.

5. Date Availability

The data that support the findings of this study are available. All data generated or analyzed during this study are included in this published article.

6. Credit Authorship Contribution Statement

Jing Zhou, Yue Li and Boyan Ren performed the experiments and analyzed the data with the help from Yutong Wei.

7. Declaration of Funding

Authors would like to appreciate the financial support from Market Supervision Administration of Sichuan Province (SCSJS2023006, SCSJ2021004), Science and Technology Department of Sichuan Province (2023YFG0252, 24LHJJ0073), Bureau of Science and Technology of Dazhou (22ZDYF0051, 21ZDYF0008), Sichuan University of Arts and Science (2022HX0020), Special Polymer Materials for Automobile Key Laboratory of Sichuan Province(22YSY-KFKT01).

8. Competing Interests

All the authors declare that they have no conflict of interest.

References

[1] El Azzouzi, M., Azzaoui, K., Warad, I., Hammouti, B., Shityakov, S., Sabbahi, R., ... & Zarrouk, A. (2022). Moroccan, Mauritania, and senegalese gum Arabic variants as green corrosion inhibitors for mild steel in HCl: Weight loss, electrochemical, AFM and XPS studies. Journal of Molecular liquids, 347, 118354.

[2] Kumar, H., & Dhanda, T. (2021). Cyclohexylamine an effective corrosion inhibitor for mild steel in 0.1 N H2SO4: experimental and theoretical (molecular dynamics simulation and FMO) study. Journal of Molecular Liquids, 327, 114847.

[3] Hegazy, M. A., El-Tabei, A. S., Bedair, A. H., & Sadeq, M. A. (2015). Synthesis and inhibitive performance of novel cationic and gemini surfactants on carbon steel corrosion in 0.5 M H_2SO_4 solution.

[4] Jeeva, M., Prabhu, G. V., Boobalan, M. S., & Rajesh, C. M. (2015). Interactions and inhibition effect of urea-derived Mannich bases on a mild steel surface in HCl. The Journal of Physical Chemistry C, 119(38), 22025-22043.

[5] Murthy, R., Gupta, P., & Sundaresan, C. N. (2020). Theoretical and electrochemical evaluation of 2-thioureidobenzheteroazoles as potent corrosion inhibitors for mild steel in 2 M HCl solution. Journal of Molecular Liquids, 319, 114081.

[6] Golchinvafa, A., Anijdan, S. M., Sabzi, M., & Sadeghi, M. (2020). The effect of natural inhibitor concentration of Fumaria officinalis and temperature on corrosion protection mechanism in API X80 pipeline steel in 1 M H2SO4 solution. International Journal of Pressure Vessels and Piping, 188, 104241.

[7] Bedair, M. A., El-Sabbah, M. M. B., Fouda, A. S., & Elaryian, H. M. (2017). Synthesis, electrochemical and quantum chemical studies of some prepared surfactants based on azodye and Schiff base as corrosion inhibitors for steel in acid medium. Corrosion science, 128, 54-72.

[8] Kalaiselvi, P., Chellammal, S., Palanichamy, S., & Subramanian, G. (2010). Artemisia pallens as corrosion inhibitor for mild steel in HCl medium. Materials Chemistry and Physics, 120(2-3), 643-648.

[9] Fakhry, H., El Faydy, M., Benhiba, F., Laabaissi, T., Bouassiria, M., Allali, M., ... & Zarrouk, A. (2021). A newly synthesized quinoline derivative as corrosion inhibitor for mild steel in molar acid medium: Characterization (SEM/EDS), experimental and theoretical approach. Colloids and Surfaces A: Physicochemical and Engineering Aspects, 610, 125746.

[10] Ehsani, A., Mahjani, M. G., Moshrefi, R., Mostaanzadeh, H., & Shayeh, J. S. (2014). Electrochemical and DFT study on the inhibition of 316L stainless steel corrosion in acidic medium by 1-(4-nitrophenyl)-5-amino-1 H-tetrazole. RSC Advances, 4(38), 20031-20037.

[11] Fernandes, C. M., Alvarez, L. X., dos Santos, N. E., Barrios, A. C. M., & Ponzio, E. A. (2019). Green synthesis of 1-benzyl-4-phenyl-1H-1, 2, 3-triazole, its application as corrosion inhibitor for mild steel in acidic medium and new approach of classical electrochemical analyses. Corrosion Science, 149, 185-194.

[12] Lgaz, H., Salghi, R., & Ali, I. H. (2018). Corrosion inhibition behavior of 9-hydroxyrisperidone as a green corrosion inhibitor for mild steel in hydrochloric acid: electrochemical, DFT and MD simulations studies. International Journal of Electrochemical Science, 13(1), 250-264.

[13] Pandey, A., Singh, B., Verma, C., & Ebenso, E. E. (2017). Synthesis, characterization and corrosion inhibition potential of two novel Schiff bases on mild steel in acidic medium. RSC advances, 7(74), 47148-47163.

[14] Gupta, R. K., Malviya, M., Verma, C., & Quraishi, M. A. (2017). Aminoazobenzene and diaminoazobenzene functionalized graphene oxides as novel class of corrosion inhibitors for mild steel: experimental and DFT studies. Materials Chemistry and Physics, 198, 360-373.

[15] Murmu, M., Saha, S. K., Murmu, N. C., & Banerjee, P. (2019). Effect of stereochemical conformation into the corrosion inhibitive behaviour of double azomethine based Schiff bases on mild steel surface in 1 mol L− 1 HCl medium: An experimental, density functional theory and molecular dynamics simulation study. Corrosion Science, 146, 134-151.

[16] Erami, R. S., Amirnasr, M., Meghdadi, S., Talebian, M., Farrokhpour, H., & Raeissi, K. (2019). Carboxamide derivatives as new corrosion inhibitors for mild steel protection in hydrochloric acid solution. Corrosion Science, 151, 190-197.

[17] Heydari, H., Talebian, M., Salarvand, Z., Raeissi, K., Bagheri, M., & Golozar, M. A. (2018). Comparison of two Schiff bases containing O-methyl and nitro substitutes for corrosion inhibiting of mild steel in 1 M HCl solution. Journal of Molecular liquids, 254, 177-187.

[18] Talebian, M., Raeissi, K., Atapour, M., Fernández-Pérez, B. M., Salarvand, Z., Meghdadi, S., ... & Souto, R. M. (2018). Inhibitive effect of sodium (E)-4-(4-nitrobenzylideneamino) benzoate on the corrosion of some metals in sodium chloride solution. Applied Surface Science, 447, 852-865.

[19] Dueke-Eze, C. U., Madueke, N. A., Iroha, N. B., Maduelosi, N. J., Nnanna, L. A., Anadebe, V. C., & Chokor, A. A. (2022). Adsorption and inhibition study of N-(5-methoxy-2-hydroxybenzylidene) isonicotinohydrazide Schiff base on copper corrosion in 3.5% NaCl. Egyptian Journal of Petroleum, 31(2), 31-37.